AdoCbl has been chemically cleaved, are not significantly different from the corrin ring conformation of base-on AdoCbl. Therefore, any change in the conformation of the corrin ring occurs only when the molecule is bound to the enzyme. To create such a large change in the conformation of the corrin ring the enzyme must be creating a large upward conformational distortion of the corrin. It has been suggested that, in AdoCbl and AdeEtCbl, the steric effect of the alkyl group prevents this upward conformational distortion from occurring without homolysis of the Co–C bond,[9] whereas it is possible with the less bulky Ade($-CH_2-$)$_n$Cbls. We believe it is possible that the adenine orientation must be correct for the distortion to occur and that this orientation is not correct for AdeEtCbl.

In conclusion, the trends observed in the enzyme binding and CD spectral changes in Ade($-CH_2-$)$_n$Cbls may not be simply a function of the bulk differences in the alkyladenine group. In addition, the orientation of the adenine ring and the fluxional character of the alkyladenine groupings probably play a role. The nucleotide loop does not appear to be affected by alkyladenine bulk or electronic properties. Although corrin ring flexibility remains a viable explanation, the X-ray and NMR results continue to point to only small changes in the corrin ring conformation in the absence of enzyme binding.

**Acknowledgment**. We are grateful for the support provided by Grants GM 29225 (to L.G.M.), CA-10925 (to J.P.G.), and CA-06927 (to I.C.R.) from the National Institutes of Health and by an appropriation from the Commonwealth of Pennsylvania (to I.C.R.). We are also grateful to Dr. Dennis Hare for the NMR processing software package used in this study, to Prof. Clark Still (Columbia University) for the MACROMODEL program, and to Cynthia Ryan for carrying out initial studies.

**Registry No.** AdePrCbl, 34502-77-7; AdeEtCbl, 59209-78-8; AdeBuCbl, 21806-90-6; AdePeCbl, 56226-23-4; hydroxocobalamin, 13422-51-0; 9-(3-chloropropyl)adenine, 19255-49-3; 9-(2-chloroethyl)adenine, 19255-48-2; 9-(4-chlorobutyl)adenine, 69293-19-2; 9-(ω-chloropentyl)-adenine, 53359-09-4.

**Supplementary Material Available**: NMR figures of the longer mixing time HOHAHA spectrum, part of the longer mixing time HOHAHA spectrum showing connectivities between the methylene protons, the short mixing time HOHAHA spectrum, part of the ROESY spectrum showing the NOE connectivities of the upfield protons, the HMQC spectrum, part of the HMBC spectrum showing the methyl proton region, and part of the HMBC spectrum showing the methine proton region, tables of anisotropic thermal parameters for all non-hydrogen atoms, fractional coordinates of hydrogen atoms, and bond distances between adjacent non-hydrogen atoms and their esd's, and an ORTEP diagram of AdePrCbl (17 pages); table of observed and calculated structure factors (41 pages). Ordering information is given on any current masthead page.

# Combined X-ray Crystallographic, Single-Crystal EPR, and Theoretical Study of Metal-Centered Radicals of the Type $\{\eta^5\text{-}C_5R_5Cr(CO)_2L\}$ (R = H, Me; L = CO, Tertiary Phosphine)

**Suzanne Fortier,*,† Michael C. Baird,*,† Keith F. Preston,*,‡ John R. Morton,*,‡ Tom Ziegler,*,§ Tilman J. Jaeger,† W. Carl Watkins,† Joseph H. MacNeil,† Kimberley A. Watson,† Kristine Hensel,† Yvon Le Page,† Jean-Pierre Charland,‡ and A. J. Williams‡**

*Contribution from the Department of Chemistry, Queen's University, Kingston, Canada K7L 3N6, Steacie Institute for Molecular Sciences, National Research Council of Canada, Ottawa, Canada K1A 0R9, and Department of Chemistry, University of Calgary, Calgary, Canada T2N 1N4.*
*Received March 26, 1990. Revised Manuscript Received September 11, 1990*

**Abstract**: The X-ray crystal structures of the compounds $\eta^5\text{-}C_5Me_5Mn(CO)_3$, $\{\eta^5\text{-}C_5Me_5Cr(CO)_2(PMe_3)\}$, and $\eta^5\text{-}C_5Me_5Mn(CO)_2(PMe_3)$, the latter two new, have been determined: $\eta^5\text{-}C_5Me_5Mn(CO)_3$ crystallizes in the centric space group $P2_1/m$, $\eta^5\text{-}C_5Me_5Mn(CO)_2(PMe_3)$ in *Pbca*, and $\{\eta^5\text{-}C_5Me_5Cr(CO)_2(PMe_3)\}$ in *Pmnb*. All three compounds assume essentially "piano-stool-like" structures, the manganese compounds with OC–Mn–CO and OC–Mn–P bond angles of $\simeq 92°$, normal for this type of 18-electron compound. In contrast, the 17-electron chromium compound exhibits a closed-in OC–Cr–CO bond angle of only 79.9 (1)°, comparable with that of the only other such compound previously reported, $\{\eta^5\text{-}C_5H_5Cr(CO)_2(PPh_3)\}$ (80.9 (1)°). Single crystals containing about 1% of $\{\eta^5\text{-}C_5Me_5Cr(CO)_3\}$ and $\{\eta^5\text{-}C_5Me_5Cr(CO)_2(PMe_3)\}$ doped into their manganese analogues have been studied by EPR spectroscopy at 20 K, and the g and $^{31}P$ hyperfine tensors have been assembled in the crystal-axis systems of the hosts. Although interpretation of the data for $\{\eta^5\text{-}C_5Me_5Cr(CO)_3\}$ is not unambiguous, $^2A''$ ground states seem likely for both it and $\{\eta^5\text{-}C_5Me_5Cr(CO)_2(PMe_3)\}$, as was observed previously for $\{\eta^5\text{-}C_5H_5Cr(CO)_2(PPh_3)\}$. Complementing the above, LCAO-HFS calculations for $\{\eta^5\text{-}C_5H_5Cr(CO)_3\}$ and $\{\eta^5\text{-}C_5H_5Cr(CO)_2(PH_3)\}$ have also been carried out, the nature and geometry-optimized structures of the ground states being determined. While $\{\eta^5\text{-}C_5H_5Cr(CO)_3\}$ is predicted to assume a $^2A'$ ground state, the first excited state, of $^2A''$ character, lies only some 7 kJ mol$^{-1}$ higher; thus both states should be populated in the gas phase, and the relative ordering in condensed media may well be sensitive to the environment. Interestingly, $\{\eta^5\text{-}C_5H_5Cr(CO)_2(PH_3)\}$ is predicted to assume a $^2A''$ ground state with an optimized geometry in which the OC–Cr–CO angle is $\simeq 80°$, in agreement with the EPR data and the X-ray crystal structures of both $\{\eta^5\text{-}C_5Me_5Cr(CO)_2(PMe_3)\}$ and $\{\eta^5\text{-}C_5H_5Cr(CO)_2(PPh_3)\}$.

Considerable interest has developed in recent years in 17-electron, organotransition-metal complexes, in large part because very little is known as yet of the chemistry and of the electronic structures of this unusual class of compounds.[1] Relevant to the present study, aspects of the chemistry of the 17-electron com-

† Queen's University.
‡ National Research Council of Canada.
§ University of Calgary.

(1) Baird, M. C. *Chem. Rev.* **1988**, *88*, 1217.

0002-7863/91/1513-542$02.50/0 

**Table I.** Crystallographic Data for η⁵-$C_5Me_5Mn(CO)_3$, η⁵-$C_5Me_5Mn(CO)_2(PMe_3)$, and {η⁵-$C_5Me_5Cr(CO)_2(PMe_3)$}

| | | | | | |
|---|---|---|---|---|---|
| | | | η⁵-$C_5Me_5Mn(CO)_3$ | | |
| formula | $C_{13}H_{15}O_3M$ | $Z$ | 2 | no. of unique reflns | 932 |
| fw | 274.20 | $D_c$, g cm$^{-1}$ | 1.362 | no. of obsvd reflns | 511 |
| cryst system | monoclinic | cryst dimns, mm$^3$ | 0.10 × 0.20 × 0.30 | $I/\sigma(I)$ ratio | 3.0 |
| space group | $P2_1/m$ | abs coeff, $\mu$, mm$^{-1}$ | 0.94 | $R_f$ | 0.051 |
| $a$, Å | 6.7518 (6) | radiation (λ, Å) | Mo Kα (0.70932) | $R_w$ | 0.050 |
| $b$, Å | 12.978 (3) | octants measured | $hkl$, $\bar{h}kl$, $h\bar{k}\bar{l}$, $\bar{h}k\bar{l}$ | $R_f$ (all reflns) | 0.099 |
| $c$, Å | 7.834 (2) | max 2θ, deg | 45 | $R_w$ (all reflns) | 0.057 |
| β, deg | 103.15 (1) | no. of reflns measd | 1969 | $S$ (GoF) | 1.7 |
| $V$, Å$^3$ | 668.45 | | | final $D$-map background | ≤0.24 e/Å$^3$ |
| | | | η⁵-$C_5Me_5Mn(CO)_2(PMe_3)$ | | |
| formula | $C_{15}H_{24}O_2PMn$ | $Z$ | 8 | no. of unique reflns | 1883 |
| fw | 322.27 | $D_c$, g cm$^{-1}$ | 1.559 | no. of obsvd reflns | 912 |
| cryst system | orthorhombic | cryst dimns, mm$^3$ | 0.15 × 0.35 × 0.45 | $I/\sigma(I)$ ratio | 3.0 |
| space group | $Pbca$ | abs coeff, $\mu$, mm$^{-1}$ | 1.03 | $R_f$ | 0.065 |
| $a$, Å | 14.72 (1) | radiation (λ, Å) | Mo Kα (0.70932) | $R_w$ | 0.069 |
| $b$, Å | 25.74 (1) | octants measured | $hkl$, $hk\bar{l}$ | $R_f$ (all reflns) | 0.065 |
| $c$, Å | 8.973 (3) | max 2θ, deg | 40 | $S$ (GoF) | 4.09 |
| $V$, Å$^3$ | 3400.8 | no. of reflns measd | 3460 | final $D$-map background | ≤0.80 e/Å$^3$ |
| | | | {η⁵-$C_5Me_5Cr(CO)_2(PMe_3)$} | | |
| formula | $C_{15}H_{24}CrO_2P$ | $Z$ | 4 | no. of unique reflns | 2528 |
| fw | 319.33 | $D_c$, g cm$^{-1}$ | 1.266 | no. of obsvd reflns | 836 |
| cryst system | orthorhombic | cryst dimns, mm$^3$ | 0.20 × 0.20 × 0.20 | $I/\sigma(I)$ ratio | 3.0 |
| space group | $Pmnb$ | abs coeff, $\mu$, mm$^{-1}$ | 0.76 | $R_f$ | 0.046 |
| $a$, Å | 12.833 (5) | radiation (λ, Å) | Mo Kα (0.70932) | $R_w$ | 0.055 |
| $b$, Å | 16.688 (7) | octants measured | $hkl$ | $R_f$ (all reflns) | 0.241 |
| $c$, Å | 7.820 (4) | maximum 2θ, deg | 60 | $S$ (GoF) | 1.768 |
| $V$, Å$^3$ | 1674.7 | no. of reflns measd | 2528 | final $D$-map background | ≤0.31 e/Å$^3$ |

pound {η⁵-$C_5H_5Cr(CO)_3$} have recently been presented,[2] including substitution reactions with tertiary phosphines, L, to form derivatives of the type {η⁵-$C_5H_5Cr(CO)_2L$}. The crystal structure of one such substituted compound, {η⁵-$C_5H_5Cr(CO)_2(PPh_3)$}, has been determined,[2a] and single-crystal EPR spectra of {η⁵-$C_5H_5Cr(CO)_3$} and {η⁵-$C_5H_5Cr(CO)_2(PPh_3)$} doped into crystals of the 18-electron, diamagnetic manganese analogues have been reported.[3]

On the basis of the low-temperature (20 K) EPR spectrum of {η⁵-$C_5H_5Cr(CO)_3$} doped into a single crystal of η⁵-$C_5H_5Mn(CO)_3$, it was suggested that the degenerate e level, of largely $3d_{xy}$ and $3d_{x^2-y^2}$ character and normally associated with complexes of the type η⁵-$C_5H_5ML_3$, is split in the case of {η⁵-$C_5H_5Cr(CO)_3$} because of a Jahn–Teller distortion. It was further deduced from the EPR spectrum that the singly occupied molecular orbital (SOMO) of {η⁵-$C_5H_5Cr(CO)_3$} is essentially of $3d_{x^2-y^2}$ character, resulting in a $^2A'$ ground state for {η⁵-$C_5H_5Cr(CO)_3$} in $C_s$ symmetry.[3a,b] This conclusion was reached because of the coincidence between the direction of one of the principal axes of the **g** tensor and the perpendicular to one of the planes $z$CrC, where $z$ is the line joining the Cr atom to the centroid of the η⁵-$C_5H_5$ ring; curiously, the $z$CrC plane was not the plane which most nearly bisected the molecule. In a subsequent study of {η⁵-$C_5H_5Cr(CO)_2(PPh_3)$},[3b,c] a plane of symmetry was imposed on the molecule on replacing a CO ligand by $PPh_3$ and a different conclusion was reached, namely that the ground state was A″, with a SOMO of predominantly $3d_{xy}$ character.

In the present investigation, we describe single-crystal EPR studies of both the recently reported 17-electron compound {η⁵-$C_5Me_5Cr(CO)_3$}[4] and of a heretofore unreported derivative, {η⁵-$C_5Me_5Cr(CO)_2(PMe_3)$}, both doped into their diamagnetic manganese analogues. In order to gain yet further insight into this interesting family of molecules, we have also carried out theoretical calculations of the electronic structures of both {η⁵-$C_5H_5Cr(CO)_3$} and {η⁵-$C_5H_5Cr(CO)_2(PH_3)$}, utilizing the Hartree–Fock–Slater (HFS) method in the implementation of Baerends et al.[5] It has been shown elsewhere that the HFS methodology can be successfully applied to organometallic complexes,[6] and all structure optimizations in the present investigation were carried out by a newly developed algorithm, based on energy gradients[7] and applied successfully in conjunction with Becke's nonlocal exchange correction[8] to organometallic systems.[9] As a necessary part of this study, we have determined and report here the X-ray crystal structures of the three compounds {η⁵-$C_5Me_5Cr(CO)_2(PMe_3)$}, η⁵-$C_5Me_5Mn(CO)_3$, and η⁵-$C_5Me_5Mn(CO)_2(PMe_3)$. We also, for purposes of comparison, consider details of the crystal structure of {η⁵-$C_5H_5Cr(CO)_2(PPh_3)$}. The structure of this compound has been only briefly discussed previously, although tables of bond lengths, bond angles, atomic coordinates, thermal parameters, and observed and calculated structure parameters were provided as supplementary information in a communication.[2a]

In keeping with previous practice,[1] in order to clearly distinguish 17- and 18-electron species, we shall hereafter enclose the chemical formulae of the former in brace brackets.

## Experimental Section

**Syntheses and X-ray Crystal Structure Determinations.** The compound {η⁵-$C_5Me_5Cr(CO)_2(PMe_3)$} was synthesized by treating the dimer, [η⁵-$C_5Me_5Cr(CO)_3]_2$,[4] with 2 equiv of $PMe_3$,[10] while the new compound η⁵-$C_5Me_5Mn(CO)_2(PMe_3)$ was synthesized by photolyzing a solution of η⁵-$C_5Me_5Mn(CO)_3$ (Strem) and $PMe_3$ in THF, as described elsewhere for similar derivatives.[11] Crystals of {η⁵-$C_5Me_5Cr(CO)_2(PMe_3)$}, η⁵-$C_5Me_5Mn(CO)_3$, and η⁵-$C_5Me_5Mn(CO)_2(PMe_3)$ suitable for X-ray crystallography were grown by sublimation. Crystals containing the two radicals {η⁵-$C_5Me_5Cr(CO)_3$} and {η⁵-$C_5Me_5Cr(CO)_2(PMe_3)$} doped into

(2) (a) Cooley, N. A.; Watson, K. A.; Fortier, S.; Baird, M. C. *Organometallics* **1986**, *5*, 2563. (b) McLain, S. J. *J. Am. Chem. Soc.* **1988**, *110*, 643. (c) Cooley, N. A.; MacConnachie, P. T. F.; Baird, M. C. *Polyhedron* **1988**, *7*, 1965.

(3) (a) Krusic, P. J.; McLain, S. J.; Morton, J. R.; Preston, K. F.; Le Page, Y. *J. Magn. Reson.* **1987**, *74*, 72. (b) Morton, J. R.; Preston, K. F.; Cooley, N. A.; Baird, M. C.; Krusic, P. J.; McLain, S. J. *J. Chem. Soc., Faraday Trans. 1* **1987**, *83*, 3535. (c) Cooley, N. A.; Baird, M. C.; Morton, J. R.; Preston, K. F.; Le Page, Y. *J. Magn. Reson.* **1988**, *76*, 325.

(4) Jaeger, T. J.; Baird, M. C. *Organometallics* **1988**, *7*, 2074.

(5) Baerends, E. J.; Ellis, D. E.; Ros, P. *Chem. Phys.* **1973**, *2*, 71.

(6) (a) Becke, A. *J. Chem. Phys.* **1982**, *76*, 6037. (b) Dunlap, B. I. *J. Phys. Chem.* **1986**, *90*, 5524.

(7) Versluis, L.; Ziegler, T. *J. Chem. Phys.* **1988**, *88*, 322.

(8) Becke, A. *J. Chem. Phys.* **1986**, *84*, 4524.

(9) (a) Ziegler, T.; Tschinke, V.; Versluis, L.; Baerends, E. J.; Ravenek, W. *Polyhedron* **1988**, *7*, 1625. (b) Ziegler, T.; Tschinke, V.; Becke, A. *J. Am. Chem. Soc.* **1987**, *109*, 1351.

(10) Jaeger, T. J.; Baird, M. C. Manuscript in preparation.

(11) King, R. B.; Efraty, A.; Douglas, W. M. *J. Organomet. Chem.* **1973**, *56*, 345.

**Table II.** Selected Bond Lengths (Å) and Angles (deg) for $\eta^5$-$C_5Me_5Mn(CO)_3$

(a) Bond Lengths

| | | | | | |
|---|---|---|---|---|---|
| Mn–C1 | 1.738 (9) | Mn–C3 | 2.130 (11) | C3–C4 | 1.412 (13) |
| Mn–C2 | 1.712 (13) | Mn–C4 | 2.137 (8) | C4–C5 | 1.362 (15) |
| C1–O1 | 1.170 (12) | Mn–C5 | 2.112 (7) | C4–C7 | 1.493 (16) |
| C2–O2 | 1.185 (16) | C3–C6 | 1.420 (19) | C5–C8 | 1.483 (14) |

(b) Bond Angles

| | | | |
|---|---|---|---|
| C1–Mn–C1′ | 90.6 (4) | C4–C3–C4′ | 106.4 (10) |
| C1–Mn–C2 | 93.0 (4) | C4–C3–C6 | 126.6 (6) |
| C3–C4–C5 | 107.8 (8) | C1′–Mn–C2 | 93.0 (4) |
| C5–C4–C7 | 128.1 (12) | C3–C4–C7 | 124.1 (11) |
| C4–C5–C8 | 128.1 (11) | C4–C5–C5′ | 109.0 (8) |
| Mn–C1–O1 | 178.0 (8) | C5′–C5–C8 | 122.6 (11) |
| Mn–C2–O2 | 177.5 (10) | | |

their manganese analogues to the extent of about 1% by weight and suitable for EPR spectroscopy were grown by co-sublimation of mixtures of pairs of the compounds, utilizing the dimer, $[\eta^5$-$C_5Me_5Cr(CO)_3]_2$, in the former case.

Crystal structure determinations of $\{\eta^5$-$C_5Me_5Cr(CO)_2(PMe_3)\}$, $\eta^5$-$C_5Me_5Mn(CO)_3$, and $\eta^5$-$C_5Me_5Mn(CO)_2(PMe_3)$ were carried out on Enraf-Nonius CAD-4 (Queen's or N.R.C.C.) diffractometers. For the compound $\eta^5$-$C_5Me_5Mn(CO)_3$, a clear yellow crystal, dimensions $\simeq$0.1 × $\simeq$0.2 × $\simeq$0.3 mm, was sealed in a glass capillary, and cell parameters and intensity measurements were performed with graphite-monochromatized Mo K$\alpha$ radiation. Accurate cell parameters were obtained from 30 well-centered reflections with $2\theta$ angles ranging from 30° to 35°. Intensity data were collected with use of the $\omega/2\theta$ scan mode, up to a $2\theta$ angle value of 45°. Details related to the crystal data and the intensity measurements are summarized in Table I. The systematic absence $0k0$, $k \neq 2n$, was noted in the data set of the compound and was consistent with two possible space groups, $P2_1$ and $P2_1/m$. After averaging symmetry-related reflections, the reflection data were corrected, as usual, for the Lorentz and polarization ratio[12] effects, but not for absorption because of the low $\mu$ value. Details pertaining to the data reduction step are listed in Table I.

The acentric space group $P2_1$ was assumed at first and the structure was solved by direct methods with MULTAN.[13] After initial block-diagonal least-squares refinement of the fractional and isotropic $U$ values of the non-hydrogen atoms and close inspection of the packing diagram, we suspected the presence of mirror planes perpendicular to the 2-fold screw axis. The possibility of extra symmetry was later confirmed by the symmetry detection routine MISSYM[14,15] which found, in addition to the 2-fold screw axis, centers of symmetry and mirror symmetry. The non-hydrogen atom coordinates of the new asymmetric unit were shifted with respect to the origin of the new cell having symmetry elements of the centric space group $P2_1/m$. Least-squares refinement was resumed as the non-hydrogen atoms were refined anisotropically. Most of the methyl hydrogen atoms were located on the next difference Fourier map. The missing hydrogen atoms were fixed at calculated positions ($sp^3$-hybridized carbon atoms and a C–H distance of 1.08 Å). All hydrogen atoms were given isotropic $U$ parameters related to the $U_{eq}$ of the carbon atom to which they were attached. The hydrogen atoms were then included in the next full-matrix least-squares cycles but their parameters were not refined. If necessary, new hydrogen atomic positions would be calculated before pursuing refinement. The final refinement parameters are listed in Table I. The weighting scheme was $w^{-1} = \sigma^2(F_o) + 0.0003F_o^2$. Neutral atom scattering factors were taken from standard sources.[16] All calculations were carried out on a VAX 11/780 with the NRCVAX system of programs.[17] Final positional and equivalent thermal parameters are deposited as Supplementary Material. Selected bond lengths and angles are given in Table II, and an ORTEP drawing is shown in Figure 1a.

For the compound $\eta^5$-$C_5Me_5Mn(CO)_2(PMe_3)$, there were difficulties in obtaining a single crystal suitable for data collection. Several specimens from two crystallization batches were examined with precession photography. A yellow crystal of dimensions $\simeq$0.15 × $\simeq$0.35 × $\simeq$0.45 mm, sealed in a glass capillary, was eventually used for data collection although it was clear from the photographs, in particular from the doubling of several reflections, that it was not of very high quality. It was nevertheless possible to determine from the photographs that the speciman crystallized in the orthorhombic space group *Pbca*. The cell parameters and intensity measurements were performed on an Enraf-Nonius CAD-4 diffractomer with graphite-monochromatized Mo K$\alpha$ radiation. The cell parameters were obtained from 25 centered reflections with $2\theta$ angles ranging from 10° to 26°. The poor quality of the crystal was apparent in the cell angles, which deviated by as much as 0.1° from the 90° value expected for orthorhombic unit cells. Intensity data were collected with use of the $\omega/2\theta$ scan mode, up to a $2\theta$ angle value of 40°. Three standard reflections were measured every 7200 s of radiation time and showed no significant variation during the course of data collection. The intensities were corrected for Lorentz and polarization effects but not for absorption. Symmetry-related reflections were collected for 1576 reflections of the unique set. The poor quality of the crystal was again apparent in the averaging of these symmetry-related reflections, which gave an agreement factor on intensity, $R_I$, of 0.13. The structure was solved by direct methods with the program MULTAN 80.[13] Difference Fourier map calculations revealed the positions of nine of the hydrogen atoms, while the positions of the others were calculated. Full-matrix least-squares refinement was carried for a scale factor and positional and anisotropic thermal parameters of the non-hydrogen atoms. The hydrogen atoms were included in the calculations but not refined. They were assigned thermal parameters equal in magnitude to that of the parent carbon atom. The function minimized was $\sum w||F_o| - |F_c||^2$ where $w^{-1} = \sigma^2(|F_o|)$. Neutral atom scattering factors were taken from standard sources.[16] All calculations were carried out on a PDP 11/23 computer using SDP, the structure determination package of Enraf-Nonius. Details relating to the crystal data, intensity measurements, and the data collection are summarized in Table I. Final positional and equivalent thermal parameters are deposited as Supplementary Material.

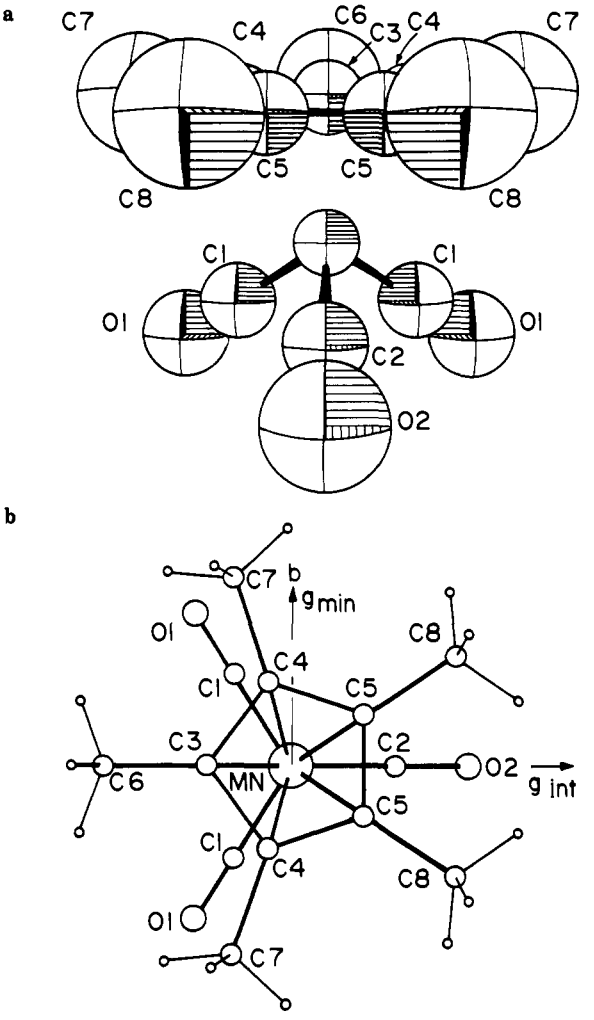


**Figure 1.** (a) ORTEP drawing of $\eta^5$-$C_5Me_5Mn(CO)_3$; (b) PLUTO drawing of $\eta^5$-$C_5Me_5Mn(CO)_3$ showing the location of the principal values of **g** for the dopant $\{\eta^5$-$C_5Me_5Cr(CO)_3\}$.

(12) Le Page, Y.; Gabe, E. J.; Calvert, L. D. *J. Appl. Crystallogr.* **1979**, *12*, 25.
(13) Germain, G.; Main, P.; Woolfson, M. M. *Acta Crystallogr.* **1971**, *A27*, 368.
(14) Charland, J. P. *Inorg. Chim. Acta* **1987**, *135*, 191.
(15) Le Page, Y. *ACA Meeting Abstr.* **1986**, *14*, 17.
(16) *International Tables for X-Ray Crystallography*, 2nd ed.; Kynoch Press: Birmingham, 1974; Vol. 4.
(17) Gabe, E. J.; Lee, F. L.; Le Page, Y. In *Crystallographic Computing 3*; Sheldrick, G., Goddard, R., Eds.; Clarendon Press: Oxford, 1985; p 167.

**Table III.** Selected Bond Lengths (Å) and Angles (deg) for $\eta^5\text{-}C_5Me_5Mn(CO)_2(PMe_3)$

| Bond Lengths | | | | | |
|---|---|---|---|---|---|
| Mn–P | 2.220 (2) | C3–C4 | 1.366 (1) | C6–C11 | 1.499 (11) |
| P–C13 | 1.810 (10) | C3–C7 | 1.301 (11) | C7–C12 | 1.558 (13) |
| P–C14 | 1.805 (9) | C3–C8 | 1.546 (12) | Mn–C3 | 2.058 (10) |
| P–C15 | 1.847 (8) | C4–C5 | 1.366 (10) | Mn–C4 | 2.104 (10) |
| Mn–C1 | 1.769 (8) | C4–C9 | 1.478 (12) | Mn–C5 | 2.158 (7) |
| Mn–C2 | 1.616 (8) | C5–C6 | 1.388 (9) | Mn–C6 | 2.152 (7) |
| C1–O1 | 1.161 (7) | C5–C10 | 1.521 (11) | Mn–C7 | 2.130 (8) |
| C2–O2 | 1.246 (9) | C6–C7 | 1.441 (11) | | |

| Bond Angles | | | |
|---|---|---|---|
| C13–P–C14 | 99.6 (4) | C5–C4–C9 | 125.6 (9) |
| C13–P–C15 | 103.2 (4) | C4–C5–C6 | 109.1 (7) |
| C14–P–C15 | 100.8 (4) | C4–C5–C10 | 126.5 (9) |
| C1–Mn–C2 | 93.0 (4) | C6–C5–C10 | 123.9 (9) |
| Mn–C1–O1 | 177.2 (7) | C5–C6–C7 | 104.6 (7) |
| Mn–C2–O2 | 180.0 (9) | C5–C6–C11 | 128.0 (9) |
| C4–C3–C7 | 111.2 (8) | C7–C6–C11 | 127 (1) |
| C4–C3–C8 | 124 (1) | C3–C7–C6 | 108.0 (7) |
| C7–C3–C8 | 124 (1) | C3–C7–C12 | 131 (1) |
| C3–C4–C5 | 107.0 (8) | C6–C7–C12 | 120 (1) |
| C3–C4–C9 | 126 (1) | | |

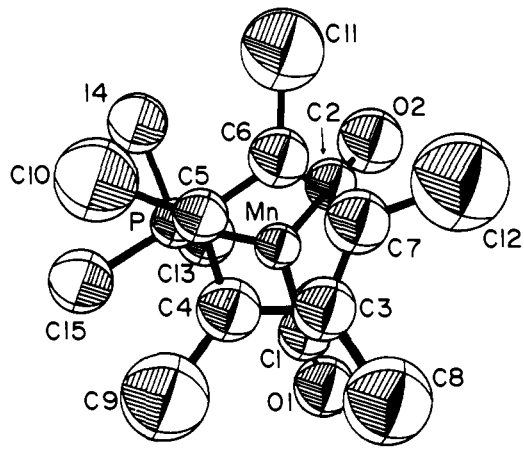


**Figure 2.** ORTEP drawing of $\eta^5\text{-}C_5Me_5Mn(CO)_2(PMe_3)$.

Selected bond lengths and angles are given in Table III, and an ORTEP drawing is shown in Figure 2.

For the compound $\{\eta^5\text{-}C_5Me_5Cr(CO)_2(PMe_3)\}$, a black crystal, dimensions $\simeq 0.20 \times \simeq 0.20 \times \simeq 0.20$ mm, was mounted in a glass capillary. Cell parameters and intensity data were measured with graphite-monochromatized Mo K$\alpha$ radiation. Accurate cell parameters were obtained from 25 well-centered reflections with $2\theta$ angles ranging from 13° to 26°. Intensity data were collected with use of the $\omega/2\theta$ scan mode, up to a $2\theta$ angle value of 60°. Three standard reflections were measured every 7200 s of radiation time and showed no significant variations during the course of data collection. The intensities were corrected for Lorentz and polarization effects but not for absorption. The structure was solved by direct methods with the program MULTAN 80.[13] Difference Fourier map calculations revealed the positions of all the hydrogen atoms. Full-matrix least-squares refinement was carried out for a scale factor and positional and anisotropic thermal parameters of the non-hydrogen atoms. The hydrogen atoms were included in the calculations but not refined. They were assigned isotropic thermal parameters equal in magnitude to that of the parent carbon atoms. The function minimized was $\sum w||F_o| - |F_c||^2$ where $w^{-1} = \sigma^2(|F_o|)$. Neutral atom scattering factors were taken from standard sources.[16] All calculations were carried out on a PDP 11/23 with SDP, the structure determination package of Enraf-Nonius. Details relating to the crystal data, intensity measurements, and the data collection are summarized in Table I. Final positional and equivalent thermal parameters are deposited as Supplementary Material. Selected bond lengths and angles are given in Table IV, and an ORTEP drawing is shown in Figure 3.

For the compound $\{\eta^5\text{-}C_5H_5Cr(CO)_2(PPh_3)\}$, a listing of observed and calculated structure factors, bond lengths, bond angles, atomic coordinates, and thermal parameters is available in the Supplementary Material of ref 2a. For purposes of comparison, however, selected bond lengths and angles are shown in Table V, and an ORTEP drawing is shown in Figure 4.

**Table IV.** Selected Bond Lengths (Å) and Angles (deg) for $\{\eta^5\text{-}C_5Me_5Cr(CO)_2(PMe_3)\}$[a]

| Bond Lengths | | | | | |
|---|---|---|---|---|---|
| Cr–C1 | 1.825 (5) | Cr–C6 | 2.223 (4) | C6–C6′ | 1.426 (8) |
| C1–O1 | 1.155 (5) | C4–C5 | 1.407 (6) | C6–C9 | 1.495 (6) |
| Cr–P | 2.345 (2) | C4–C7 | 1.514 (9) | P–C2 | 1.822 (5) |
| Cr–C4 | 2.167 (6) | C5–C6 | 1.388 (6) | P–C3 | 1.823 (6) |
| Cr–C5 | 2.187 (4) | C5–C8 | 1.512 (6) | | |

| Bond Angles | | | |
|---|---|---|---|
| C1–Cr–P | 91.5 (1) | Cr–P–C2 | 118.1 (2) |
| C1–Cr–C1′ | 79.7 (3) | Cr–P–C3 | 113.8 (2) |
| C5–C4–C5′ | 107.6 (5) | C2–P–C2′ | 102.3 (4) |
| C4–C5–C6 | 108.4 (4) | C2–P–C3 | 100.9 (2) |
| C5–C6–C6′ | 107.7 (3) | | |

[a] The primed and unprimed atoms are mutually related by the symmetry operation $^1/_2 - x, y, z$.

**Table V.** Selected Bond Lengths (Å) and Angles (deg) for $\{\eta^5\text{-}C_5H_5Cr(CO)_2(PPh_3)\}$

| (a) Bond Distances | | | | | |
|---|---|---|---|---|---|
| Cr–C1 | 1.826 (3) | Cr–C6 | 2.210 (3) | C3–C4 | 1.38 (12) |
| Cr–C2 | 1.816 (4) | Cr–C7 | 2.199 (3) | C4–C5 | 1.39 (12) |
| Cr–C3 | 2.193 (3) | Cr–P | 2.345 (1) | C3–C7 | 1.40 (12) |
| Cr–C4 | 2.185 (3) | C1–O1 | 1.16 (12) | C5–C6 | 1.36 (12) |
| Cr–C5 | 2.193 (4) | C2–O2 | 1.16 (12) | C6–C7 | 1.37 (12) |

| (b) Bond Angles | | | |
|---|---|---|---|
| C1–Cr–C2 | 80.9 (1) | Cr–C1–O1 | 175.8 (1) |
| P–Cr–C1 | 93.3 (1) | Cr–C2–O2 | 177.3 (1) |
| P–Cr–C2 | 93.4 (1) | C3–C4–C5 | 108.2 (1) |
| C4–C3–C7 | 107.3 (1) | C4–C5–C6 | 107.6 (1) |
| C5–C6–C7 | 109.5 (1) | C3–C7–C6 | 107.2 (1) |
| Cr–P–C11 | 114.42 (9) | Cr–P–C21 | 115.11 (9) |
| Cr–P–C31 | 115.4 (1) | C11–P–C21 | 102.7 (1) |
| C11–P–C31 | 104.5 (1) | C21–P–C31 | 103.2 (1) |

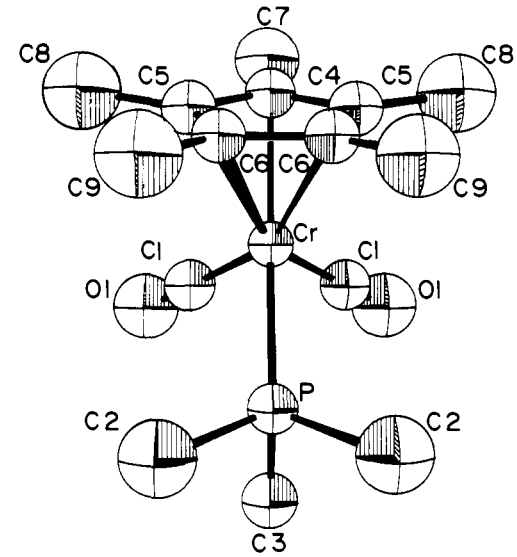


**Figure 3.** ORTEP drawing of $\{\eta^5\text{-}C_5Me_5Cr(CO)_2(PMe_3)\}$.

**EPR Studies.** EPR spectra were recorded and measured with a Varian E12 spectrometer equipped with a Bruker ER 035M NMR gaussmeter and a Systron-Donner microwave frequency counter. Temperature control was achieved with an Oxford Instruments liquid helium cryostat in the range 4–100 K, and with a gaseous nitrogen cryostat in the range 90–300 K. Single-crystal specimens were selected with the aid of a polarizing microscope and were held and oriented within the rectangular resonant microwave cavity of the spectrometer with a one-circle[3a] or a two-circle goniometer.[18]

Initial examination by EPR spectroscopy for random orientations of the dc magnetic field of crystals of $\eta^5\text{-}C_5Me_5Mn(CO)_3$ and $\eta^5\text{-}C_5Me_5Mn(CO)_2(PMe_3)$ doped with their chromium analogues showed "site behavior"[18] consistent with the space groups of the undoped crystals,

(18) Morton, J. R.; Preston, K. F. *J. Magn. Reson.* **1983**, *52*, 457.

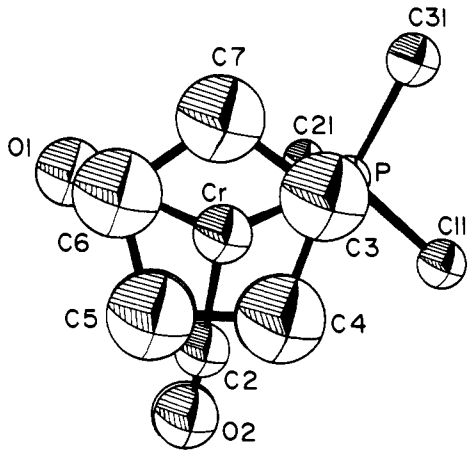


Figure 4. Structure of $\{\eta^5\text{-}C_5H_5Cr(CO)_2(PPh_3)\}$. (Phenyl rings omitted for reasons of clarity).

Table VI. The $\mathbf{g}^2$ Tensor of $\{\eta^5\text{-}C_5Me_5Cr(CO)_3\}$ Trapped in a Single Crystal of $\eta^5\text{-}C_5Me_5Mn(CO)_3$[a]

| tensor of $\mathbf{g}^2$ in $abc^*$ axes | | | principal values of $\mathbf{g}^2$ and $\mathbf{g}$ and their directional cosines | | |
|---|---|---|---|---|---|
| | | | $\mathbf{g}^2 = 3.9892$ $\mathbf{g} = 1.9973$ | $\mathbf{g}^2 = 4.0770$ $\mathbf{g} = 2.0192$ | $\mathbf{g}^2 = 4.5006$ $\mathbf{g} = 2.1215$ |
| 4.4736 | 0.0000 | −0.1034 | 0.0000 | 0.2523 | 0.9677 |
| 0.0000 | 3.9892 | 0.0000 | 1.0000 | 0.0000 | 0.0000 |
| −0.1034 | 0.0000 | 4.1040 | 0.0000 | 0.9677 | −0.2523 |

[a] The axis system is $abc^*$.

$P2_1/m$ and $Pbca$, respectively. Since monoclinic $\eta^5\text{-}C_5Me_5Mn(CO)_3$ showed only a single site spectrum, it was necessary to prealign the doped crystals by X-ray diffractometry[3a] using the known crystal structure. Accordingly, single crystals of the material were aligned and glued to a 4 mm o.d. quartz tube such that each of the monoclinic $a$, $b$, and $c^*$ axes in turn lay along the tube axis; a pointer attached to the tube indicated the direction of a second crystal axis in the perpendicular plane. Crystals so mounted were held in the helium cryostat at the center of the spectrometer resonant cavity such that the pointer lay flush with a horizontal brass protractor marked in 5° intervals. Rotation of the crystal about the vertical tube axis caused the dc magnetic field to explore one of the crystal planes $ab$, $ac^*$, or $bc^*$. Spectra were recorded and measured at 10° intervals throughout each of the planes at a temperature of 20 K.

Since doped crystals of $\eta^5\text{-}C_5Me_5Mn(CO)_2(PMe_3)$ showed anisotropic behavior characteristic of the presence of four magnetically inequivalent sites, and since the spectrum did not broaden significantly upon warming to the temperature of liquid nitrogen, it was possible to use a two-circle goniometer and the method of spectral coalescences[18] (at 90 K) to determine the $\mathbf{g}$ tensor in the crystal-axis system. Three mutually orthogonal directions were found within the crystal for which the EPR spectrum coalesced to a pair of lines separated by 30 G. No simpler spectra were observed for any orientation; indeed, for many orientations the spectra consisted of eight lines. Comparison with crystals oriented by X-ray diffractometry confirmed the location of the orthorhombic crystal axes and permitted labeling. Spectra were subsequently obtained at 10° intervals for each of the three crystal planes, $ab$, $ac$, and $bc$. Goniometer readings for each required orientation were generated with a computer program.[19]

Values of $g^2$ were calculated and plotted against angle (Figures 5 and 6) for each of the crystal planes. In the case of $\eta^5\text{-}C_5Me_5Mn(CO)_2(PMe_3)$ crystals, the $g$ value was calculated from the average of the magnetic field intensity measurements for the two components of the $^{31}P$ doublet of each site. Least-squares procedures were used to obtain the best-fit diagonal and off-diagonal $\mathbf{g}^2$-matrix elements (Tables VI and VII) for the $\{\eta^5\text{-}C_5Me_5Cr(CO)_3\}$ and $\{\eta^5\text{-}C_5Me_5Cr(CO)_2(PMe_3)\}$ radicals in their Mn-analogue host crystal-axis systems. In the case of the orthorhombic crystal, sign ambiguity among the off-diagonals of the tensor was resolved from measurements made for $B_0$ parallel to the skew direction $(1/\sqrt{3}, 1/\sqrt{3}, 1/\sqrt{3})$.[18]

**Theoretical Calculations.** HFS calculations were performed on a Cyber-205 computer (Calgary) utilizing the LCAO–HFS program system of Baerends et al.;[5] the exchange parameter $\alpha_{ex}$ was given a standard value of 7. An uncontracted triple $\zeta$-STO basis set[20] was employed for chromium, whereas the ligand atoms were represented by a double-$\zeta$ STO basis set.[20] The phosphorus basis was augmented by a 3d polarization function. All metal–ligand bond distances were taken from the relevant crystallographic data presented herein and elsewhere,[2a] while the geometry optimizations were carried out by means of the newly developed energy gradient algorithm[7] for the remaining degrees of freedom.

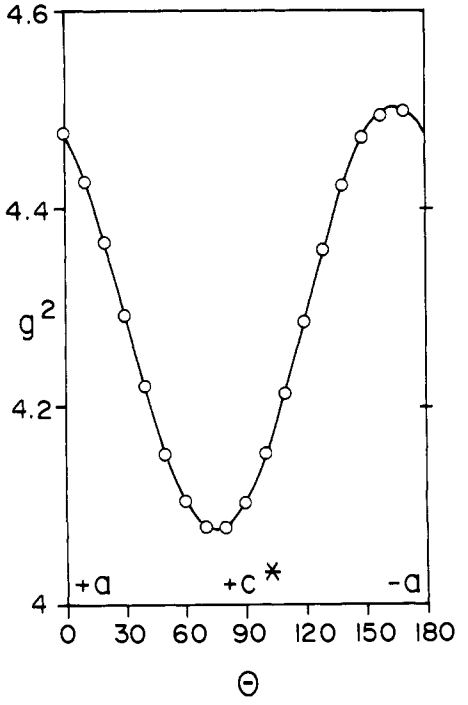


Figure 5. Experimental (circles) $g^2$ values and best-fit sinusoidal curve in the $ac$ plane at 20 K for $\{\eta^5\text{-}C_5Me_5Cr(CO)_3\}$ in $\eta^5\text{-}C_5Me_5Mn(CO)_3$.

## Results and Discussion

**Descriptions of the Crystal Structures.** Figure 1a shows an ORTEP drawing of $\eta^5\text{-}C_5Me_5Mn(CO)_3$; the "piano-stool" structure is apparent. The compound, which exists as discrete molecules in the crystal, possesses mirror symmetry with the Mn atom, the C2–O2 carbonyl group, and the C3–C6H$_3$ fragment of the five-membered ring located on the mirror plane. A similar arrangement was also found in the crystal structure of $\eta^5\text{-}C_5H_5Mn(CO)_3$,[21] although the Mn–C bonds are slightly longer in the latter compound. The molecules of $\eta^5\text{-}C_5Me_5Mn(CO)_3$, which propagate along the mirror planes of the unit cell at $y = {}^1/_4$ and ${}^3/_4$, exhibit Mn–$C_5Me_5$ ring centroid directions which are ≈10° and ≈113° away from the $a$ and $c$ axes, respectively.

An ORTEP drawing of $\eta^5\text{-}C_5Me_5Mn(CO)_2(PMe_3)$ is shown in Figure 2. As can be seen, the compound adopts a "piano-stool" structure in which the Mn–P bond axis eclipses a ring carbon atom of the $C_5Me_5$ ring. The structure is very similar to those of $\eta^5\text{-}C_5H_5Mn(CO)_3$ and $\eta^5\text{-}C_5Me_5Mn(CO)_3$, although the relatively low quality of the data, mentioned above, renders invalid any detailed quantitative comparisons.

An ORTEP drawing of $\{\eta^5\text{-}C_5Me_5Cr(CO)_2(PMe_3)\}$ is shown in Figure 3, where the mirror plane of the molecule in the crystal is readily apparent. As can be seen, the compound is monomeric (shortest Cr–Cr distance 6.772 (1) Å) and adopts a "piano-stool" structure very similar to that of $\{\eta^5\text{-}C_5H_5Cr(CO)_2(PPh_3)\}$[2a] (Table IV, Figure 4) and to those of the two manganese compounds under consideration here and shown in Figures 1 and 2. In contrast to $\eta^5\text{-}C_5Me_5Mn(CO)_2(PMe_3)$ but similar to $\{\eta^5\text{-}C_5H_5Cr(CO)_2(PPh_3)\}$,[2a] however, the structure of $\{\eta^5\text{-}C_5Me_5Cr(CO)_2(PMe_3)\}$

(19) Morton, J. R.; Preston, K. F.; Strach, S. J. *Rev. Sci. Instrum.* **1981**, *52*, 1358.

(20) (a) Snijders, J. G.; Vernoojis, P.; Baerends, E. J. *At. Data Nucl. Data Tables* **1981**, *26*, 483. (b) Vernoojis, P.; Snijders, J. G.; Baerends, E. J. *Slater Type Basis Functions for the Whole Periodic System*; Internal Report, Free University: The Netherlands, 1981.

(21) Berndt, A. F.; Marsh, R. E. *Acta Crystallogr.* **1963**, *16*, 118.

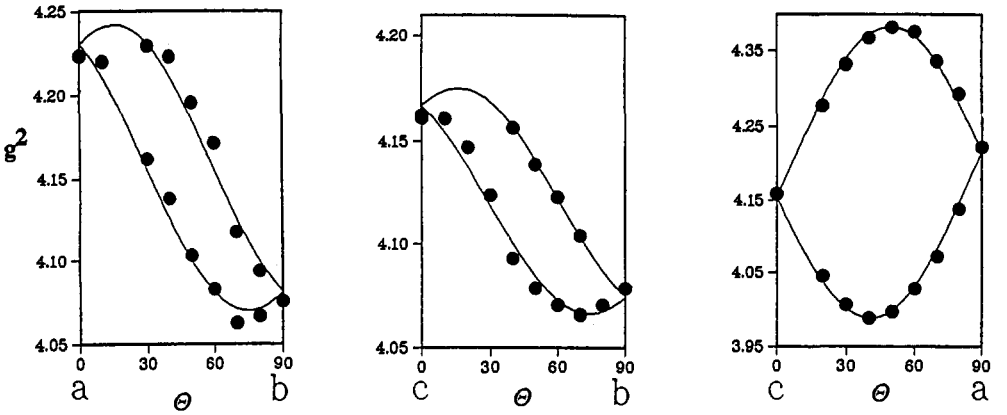


**Figure 6.** Experimental $g^2$ values and best-fit sine curves for $\{\eta^5\text{-}C_5Me_5Cr(CO)_2(PMe_3)\}$ at 90 K for the three crystal planes of $\eta^5\text{-}C_5Me_5Mn(CO)_2(PMe_3)$.

**Table VII.** The $\mathbf{g}^2$ Tensor of $\{\eta^5\text{-}C_5Me_5Cr(CO)_2(PMe_3)\}$ Trapped in a Single Crystal of $\eta^5\text{-}C_5Me_5Mn(CO)_2(PMe_3)$[a]

| | $\mathbf{g}^2$ tensor[b] | | | principal values of $\mathbf{g}^2$ and $\mathbf{g}$ and their directional cosines | | |
|---|---|---|---|---|---|---|
| | *a* | *b* | *c* | $g^2 = 3.9921$ $g = 1.9980$ | $g^2 = 4.0731$ $g = 2.0182$ | $g^2 = 4.3960$ $g = 2.0967$ |
| | 4.221 | 0.433 | −0.1949 | 0.6535 | 0.0656 | 0.7540 |
| | 0.0433 | 4.0807 | −0.0276 | −0.0851 | −0.9836 | 0.1593 |
| | −0.1949 | −0.0276 | 4.1584 | 0.7521 | −0.1683 | −0.6372 |
| | | | Crystal Directions | | | |
| (1) | 0.7087 | −0.0276 | 0.7050 | ⊥ to plane Mn–P–$C_7$ | | 5.3° from $g_{xx}$ |
| (2) | 0.7383 | 0.1279 | −0.6622 | Mn–ring centroid | | 2.4° from $g_{zz}$ |
| (3) | 0.1374 | −0.9883 | −0.0665 | $C_7$–ring centroid | | 7.2° from $g_{yy}$ |
| (4) | 0.0720 | −0.9912 | −0.1112 | cross-product (2) × (1) | | 3.3° from $g_{yy}$ |

[a] Principal values, principal directions, and certain direction cosines in the orthorhombic crystal axis system *a*, *b*, and *c*. [b] Tensor off-diagonals for one of four sites; other tensors obtained by taking all off-diagonals to be positive, or any pair of equal off-diagonals to be positive, the others negative.

exhibits an OC–Cr–CO bond angle of only 79.9 (1)°, much smaller than the approximately 90° bond angles normally found for 18-electron compounds of similar stoichiometries. The other major difference between the structures of $\{\eta^5\text{-}C_5Me_5Cr(CO)_2(PMe_3)\}$ and $\eta^5\text{-}C_5Me_5Mn(CO)_2(PMe_3)$ is the orientation of the $\eta^5\text{-}C_5Me_5$ rings relative to the rest of the molecule. In the case of the chromium compound, the Cr–P bond eclipses an edge of the $C_5Me_5$ ring while, for the manganese compound, the Mn–P bond eclipses a carbon atom of the $C_5Me_5$ ring, as pointed out above. Since differences in the analogous interatomic distances are subtle and appear only to reflect expected differences in the metal atomic radii, it is presumably the difference in the orientations of the $\eta^5\text{-}C_5Me_5$ rings which induces the two compounds to crystallize in different space groups. The differences are probably not a result of some subtle but significant difference in the electronic structures of the two compounds, since the $\eta^5\text{-}C_5H_5$ ring of $\{\eta^5\text{-}C_5H_5Cr(CO)_2(PPh_3)\}$ is oriented as in $\eta^5\text{-}C_5Me_5Mn(CO)_2(PMe_3)$ (see below). We also note that there is no evidence of ring slippage in either of the compounds $\{\eta^5\text{-}C_5Me_5Cr(CO)_2(PMe_3)\}$ or $\{\eta^5\text{-}C_5H_5Cr(CO)_2(PPh_3)\}$; although the chromium–$C_5$ ring distances and the ring carbon–carbon distances do vary somewhat, there is no pattern common to the two compounds.

**EPR Spectroscopic Studies.** The EPR spectrum at 20 K of $\{\eta^5\text{-}C_5Me_5Cr(CO)_3\}$ doped into single crystals of $\eta^5\text{-}C_5Me_5Mn(CO)_3$ consisted of a single line for all orientations of the dc magnetic field, no splitting due to hyperfine coupling being observed. Unfortunately, $^{53}Cr$ hyperfine satellites were so weak in the crystal spectra of all but $\{\eta^5\text{-}C_5H_5Cr(CO)_3\}$ that they were only detectable for a very limited number of directions. Thus it was not possible to assemble the corresponding metal-hyperfine tensors for the other three species. The absence of splittings due to magnetically nonequivalent sites shows that one principal *g* value lies parallel to the *b* axis of the monoclinic crystal[18] and that only the *ac** and *c***a* off-diagonal elements of the **g** tensor can be non-zero. In Figure 5 we show a plot of experimental $g^2$ values versus angular departure from +*a* in the *ac** plane, together with the least-squares best-fit sine curve for the data. The *ac** off-diagonal derived from that fit, the remaining diagonal elements of the $\mathbf{g}^2$ matrix, and the principal values and directions of **g** are given in Table VI.

**Table VIII.** Comparison of EPR Parameters for the Four Chromium-Centered Radicals

| compd | $g_{xx}$ | $g_{yy}$ | $g_{zz}$ | $a_{iso}(^{31}P)$[a] |
|---|---|---|---|---|
| $\{\eta^5\text{-}C_5H_5Cr(CO)_3\}$ | 2.0353 | 1.9969 | 2.1339 | |
| $\{\eta^5\text{-}C_5Me_5Cr(CO)_3\}$ | 1.9973 | 2.0192 | 2.1215 | |
| $\{\eta^5\text{-}C_5H_5Cr(CO)_2(PPh_3)\}$ | 1.9933 | 2.0170 | 2.1060 | 95 |
| $\{\eta^5\text{-}C_5Me_5Cr(CO)_2(PMe_3)\}$ | 1.9980 | 2.0182 | 2.0967 | 109 |

[a] Isotropic $^{31}P$ hyperfine interaction in MHz. Tensors are nearly isotropic.

The similarity (Table VIII) of the principal values of the **g** tensor of $\{\eta^5\text{-}C_5Me_5Cr(CO)_3\}$ in $\eta^5\text{-}C_5Me_5Mn(CO)_3$ to those of $\{\eta^5\text{-}C_5H_5Cr(CO)_3\}$[3a,b] confirms the assignment to $\{\eta^5\text{-}C_5Me_5Cr(CO)_3\}$. Furthermore, the close correspondence of the principal directions of its **g** tensor with certain directions in the host lattice convinces us that the dopant radical substitutes for the host molecule in the crystal. From the atomic coordinates of the $\eta^5\text{-}C_5Me_5Mn(CO)_3$ molecule, we calculate that the vector from Mn to the centroid of the $C_5Me_5$ ring is (−0.9855, 0.0000, 0.1699), which lies only 5° from the direction of the maximum *g* value, $g_{max}$. Minimum *g*, $g_{min}$, lies along *b*, the perpendicular to the crystallographic mirror plane (Figure 1b), and intermediate *g*, $g_{int}$, lies less than 1° from the $C_3$–$C_6$ bond. The observation of a single site for the radical in its monoclinic host and the implication that one of the components of **g** *must* lie along *b* show that the radical adopts the local site symmetry of the host, i.e. $C_s$. The *ac* plane is a crystallographic mirror plane which (Figure 1b) also bisects the $\eta^5\text{-}C_5Me_5Mn(CO)_3$ molecule. One principal *g* value of the substitutional radical, in this case $g_{min}$, is forced to lie perpendicular to the mirror plane, but there are no such symmetry arguments for the placement of the other two principal *g* values, $g_{int}$ and $g_{max}$. Their alignment close to $C_3$–$C_6$ and Mn–$C_5Me_5$ centroid is in response to electronic requirements, as discussed below.

The EPR spectrum of $\{\eta^5\text{-}C_5Me_5Cr(CO)_2(PMe_3)\}$ doped into a crystal of $\eta^5\text{-}C_5Me_5Mn(CO)_2(PMe_3)$ consisted of between one and four ≅40 G doublets, depending on the orientation of the dc magnetic field. The doublet separation, which showed very little directional dependence, is attributed to a nearly isotropic hyperfine interaction of the unpaired electron with a single $^{31}P$ ($I = {}^1/_2$) nucleus. The observation of spectra attributable to four magnetically distinguishable sites indicated that the **g** tensor lay skew in the orthorhombic crystal axis system. Each crystal plane showed site splitting, and plots of $g^2$ against angle were sinusoidal (Figure 6). Least-squares fitting procedures led to the elements of the $\mathbf{g}^2$ matrix given in Table VII, and subsequent numerical diagonalization yielded the principal values and directions of **g**.

The close similarity of the principal values of **g** and the isotropic $^{31}P$ hyperfine interaction (Table VIII) to those for the $\{\eta^5\text{-}C_5H_5Cr(CO)_2(PPh_3)\}$ radical[3b,c] shows that the radical present in doped $\eta^5\text{-}C_5Me_5Mn(CO)_2(PMe_3)$ is in fact $\{\eta^5\text{-}C_5Me_5Cr(CO)_2(PMe_3)\}$. A close correspondence exists between the principal directions of **g** and certain directions within the host structure, showing once again that the free radical is a substitutional impurity which adopts the symmetry of its diamagnetic manganese analogue. The $\eta^5\text{-}C_5Me_5Mn(CO)_2(PMe_3)$ host molecule has a near plane of symmetry containing the Mn, P, and $C_7$ atoms (Figure 2), and $g_{min}$ lies only 5° from the perpendicular to that plane (Table VII). Moreover, $g_{max}$ lies only 2° from the line between the manganese and the $C_5Me_5$ centroid, and $g_{int}$ lies 3° from the vector product of that direction and the perpendicular to $MnPC_7$ (7° from the line joining $C_7$ to the center of the ring). Unlike the case of $\{\eta^5\text{-}C_5Me_5Cr(CO)_3\}$ in its manganese host (see above), there are no local site symmetry elements to impose restrictions on the principal directions of the tensor. Nevertheless, the radical evidently adopts the orientation of the host molecule and its pseudo-$C_s$ symmetry. Furthermore, as is the case with the radicals $\{\eta^5\text{-}C_5H_5Cr(CO)_2(PPh_3)\}$ and $\{\eta^5\text{-}C_5Me_5Cr(CO)_3\}$, the minimum principal $g$ value is aligned perpendicular to a natural mirror plane of the molecule.

We have now measured **g** tensors for four very similar 17-electron, chromium-centered radicals in their manganese analogue hosts, $\{\eta^5\text{-}C_5H_5Cr(CO)_3\}$, $\{\eta^5\text{-}C_5Me_5Cr(CO)_3\}$, $\{\eta^5\text{-}C_5H_5Cr(CO)_2(PPh_3)\}$, and $\{\eta^5\text{-}C_5Me_5Cr(CO)_2(PMe_3)\}$. In addition, the $^{53}Cr$ hyperfine interaction tensor has been established for the first species and the $^{31}P$ hyperfine interaction tensors for the last two. The **g**-tensor components are very similar to each other; for each compound, the smallest component exhibits a value slightly less than that of a free spin (2.0023), while the other two exceed the free-spin value considerably (Table VIII). A **g** tensor of this type is anticipated[22,23] for a low-spin $d^5$ ion in a distorted octahedral environment in which the upper, empty $e_g$ pair of orbitals is remote from the three partially filled $t_{2g}$ orbitals. By treating the $\eta^5\text{-}C_5H_5$ ligand as equivalent to three facially oriented carbonyl groups[24] and transforming to a trigonal axis system, we were able to offer an explanation of the magnitude and directions of the **g** and $^{53}Cr$ hyperfine interaction tensors for $\{\eta^5\text{-}C_5H_5Cr(CO)_3\}$ in terms of a closely spaced, trigonal set of occupied d orbitals[25] for the radical.[3a] Our present theoretical calculations (see below) confirm the large magnitude of the ligand field splitting (the SOMO–LUMO gap), as well as the close spacing of the erstwhile $t_{2g}$ set of d orbitals. It is the latter near degeneracy and the attendant efficient spin relaxation which render the EPR spectrum undetectably broad except at low temperature; it also poses problems in the interpretation of the experimental **g** and metal hyperfine tensors. It is doubtful if the usual approximations[26] normally used in the interpretation of $g$ shifts and hyperfine tensors are valid in such a situation, and the excellent agreement between predicted and observed tensor elements in our original[3] considerations of $\{\eta^5\text{-}C_5H_5Cr(CO)_3\}$ is probably fortuitous. Our treatment has, in fact, been criticized[27] for the omission of off-diagonal terms in the tensors implied by the particular choice[25] of chromium d orbitals. Symmetry arguments remain valid, however, and the present discussion will rely upon them; quantitative evaluation of the tensor elements must await a full theoretical treatment.

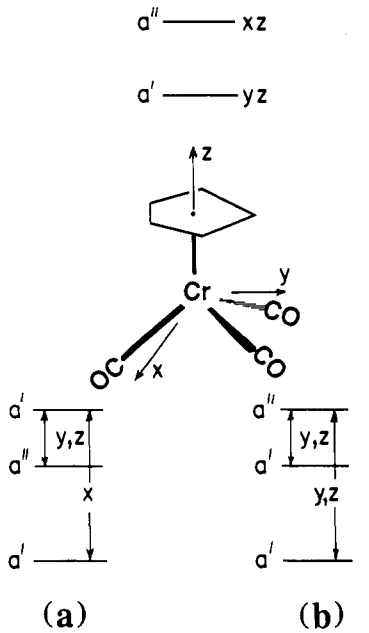


Figure 7. Possible d orbital energy level schemes for (a) $\{\eta^5\text{-}C_5H_5Cr(CO)_3\}$ and (b) for $\{\eta^5\text{-}C_5Me_5Cr(CO)_3\}$, $\{\eta^5\text{-}C_5Me_5Cr(CO)_2(PMe_3)\}$, and $\{\eta^5\text{-}C_5H_5Cr(CO)_2(PPh_3)\}$. Symmetry-allowed spin–orbital coupling between levels is indicated by vertical arrows between the levels together with the directions, e.g. $y$, $z$, of the magnetic field for which $g$ shifts from free spin are permitted.

The most striking feature common to all four free radicals is the close alignment of the maximum $g$ value, $g_{max}$, with the direction from the chromium to the centroid of the $C_5$ ring (Figure 7). That direction ($z$) is *not*, however, a symmetry element in any of the radicals, since none of them possesses strictly axial symmetry. Although species of the type $\eta^5\text{-}C_5H_5M(CO)_3$ are often treated as axially symmetric,[24,28-31] the distinctly rhombic nature of the **g** tensors of $\{\eta^5\text{-}C_5H_5Cr(CO)_3\}$ and $\{\eta^5\text{-}C_5Me_5Cr(CO)_3\}$ shows that such an assumption is unjustified for these complexes in the solid state. It has also been established that **g** and **a**($^{53}Cr$) are parallel to within 10° in $\{\eta^5\text{-}C_5H_5Cr(CO)_3\}$, and that the direction of maximum $^{53}Cr$ hyperfine interaction is close to the line between the chromium and the $C_5H_5$ centroid.[3a] This near coincidence may not, of course, occur for the other three species, for which the metal hyperfine tensors have not been established.

The close alignment of **g** and **a** tensors is certainly not anticipated by the usual[26] treatment of the trigonal basis set of d orbitals, which leads[32] to quite large off-diagonal hyperfine tensor elements. The fault may lie not so much in the choice of orbitals as in the approximations inherent in the usual assumption of nearly complete quenching of angular momentum. In view of the proximity of the three occupied orbitals indicated by our own calculations (see below), the approach taken by Bleaney and O'Brien in their elegant treatise[22] is probably more nearly correct. Using their method, we derive values for their[22] parameters of

(22) Bleaney, B.; O'Brien, M. C. M. *Proc. Phys. Soc.* **1956**, *B69*, 1216.
(23) McGarvey, B. R. *Trans. Met. Chem.* **1966**, *3*, 89.
(24) Albright, T. A.; Burdett, J. K.; Whangbo, M.-H. *Orbital Interactions in Chemistry*; Wiley-Interscience: New York, 1985; Chapter 20.
(25) Ballhausen, C. J. *Introduction to Ligand Field Theory*; McGraw-Hill: New York, 1962.
(26) Goodman, B. A.; Raynor, J. B. *Adv. Inorg. Chem. Radiochem.* **1970**, *13*, 135.
(27) Pike, R. D.; Rieger, A. L.; Rieger, P. H. *J. Chem. Soc., Trans. Faraday I* **1989**, *85*, 3913.
(28) Orgel, L. E. *J. Inorg. Nucl. Chem.* **1956**, *2*, 315.
(29) Lichtenberger, D. L.; Fenske, R. F. *J. Am. Chem. Soc.* **1976**, *98*, 50.
(30) Elian, M.; Chen, M. M. L.; Mingos, D. M. P.; Hoffmann, R. *Inorg. Chem.* **1976**, *15*, 1148.
(31) Schilling, B. E. R.; Hoffmann, R.; Lichtenberger, D. L. *J. Am. Chem. Soc.* **1979**, *101*, 585.
(32) Peake, B. M.; Rieger, P. H.; Robinson, B. H.; Simpson, J. *J. Am. Chem. Soc.* **1980**, *102*, 156.

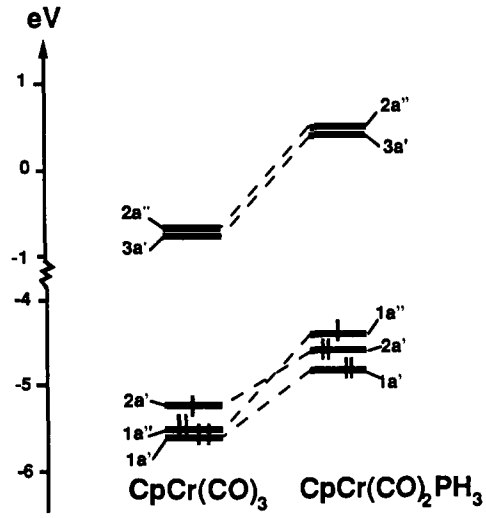


Figure 8. Calculated orbital energies for the highest occupied and lowest unoccupied valence levels in $\{\eta^5\text{-}C_5H_5Cr(CO)_3\}$ and $\{\eta^5\text{-}C_5H_5Cr(CO)_2(PH_3)\}$.

$\alpha = 34.5°$, $\theta = 0.2°$, and $k = 1.04$ from the $g$ values of $\{\eta^5\text{-}C_5H_5Cr(CO)_3\}$. The small value of $\theta$ necessarily implies near coincidence of the **g** and **a** tensors.[22]

A second feature of the principal directions of **g** is that, in three of the four radicals, $g_{min}$ lies perpendicular to a mirror (or pseudo-mirror) plane of the host. In the case of $\{\eta^5\text{-}C_5Me_5Cr(CO)_3\}$, the crystallographic mirror plane, which is also a molecular mirror plane (Figure 1), imposes such a condition upon one direction of **g**; in the cases of the two phosphine-substituted radicals, the near mirror planes containing metal, phosphorus, and $C_5$ ring centroid evidently impose a similar condition. In the case of the parent radical $\{\eta^5\text{-}C_5H_5Cr(CO)_3\}$, however, there was no correlation with the "best" pseudo-mirror plane of the host,[3a] and it appeared that this radical adopted another near-mirror plane, perpendicular to $g_{int}$ rather than $g_{min}$. Our initial reaction to this observation was to suggest that the upper two occupied orbitals (Figure 7) interchanged when a carbonyl group was replaced with a tertiary phosphine.[3b,c] Our present theoretical calculations (see below) certainly support this contention (Figures 8 and 9), as do the $g$ values themselves, which distinguish the parent radical from the others (Table VIII).

The experimental distinction between the two possible ground states, A′ and A″ in $C_s$ symmetry, is quite subtle. When $B_0 \| x$, spin orbital interaction with filled levels is symmetry forbidden for the $^2$A″ ground state (Figure 7b) but allowed for $^2$A′ (Figure 7a). In the former case, therefore, we anticipate that $x$, the perpendicular to the mirror plane, will be the direction of minimum $g$, as observed for three of the four chromium radicals. For the $^2$A′ case, symmetry arguments alone do not permit an ordering of the $g$ values, which will depend on the precise composition of the d orbitals. For the particular choice of a trigonal basis set, we showed[3a] that the intermediate $g$ value would be expected to lie along $x$ in the $^2$A′ case. From the correlation of the direction of $g_{int}$ with the perpendicular to a plane, albeit not to the "best" mirror plane, we inferred a totally symmetric ground state for $\{\eta^5\text{-}C_5H_5Cr(CO)_3\}$. Clearly this conclusion must be treated with caution, even though the inference agrees with the results of our theoretical calculations (see below). In summary, the single-crystal EPR spectroscopic results point quite clearly to a common $^2$A″ ground state for the radicals $\{\eta^5\text{-}C_5Me_5Cr(CO)_3\}$, $\{\eta^5\text{-}C_5H_5Cr(CO)_2(PPh_3)\}$, and $\{\eta^5\text{-}C_5Me_5Cr(CO)_2(PMe_3)\}$ and suggest that, exceptionally, the radical $\{\eta^5\text{-}C_5H_5Cr(CO)_3\}$ has a $^2$A′ ground state.

Independent of the choice of a′ ($d_{x^2-y^2}$) or a″ ($d_{xy}$) for the SOMO, the two levels are interconnected by the spin–orbit interaction when the dc magnetic field is along $z$ (Figure 7). The $g$ shift along $z$ is large and positive in both cases because the a′–a″ separation is small if the distortion from axial symmetry is small. Without knowing the precise atomic orbital composition of the molecular orbitals, we can only estimate an order of magnitude

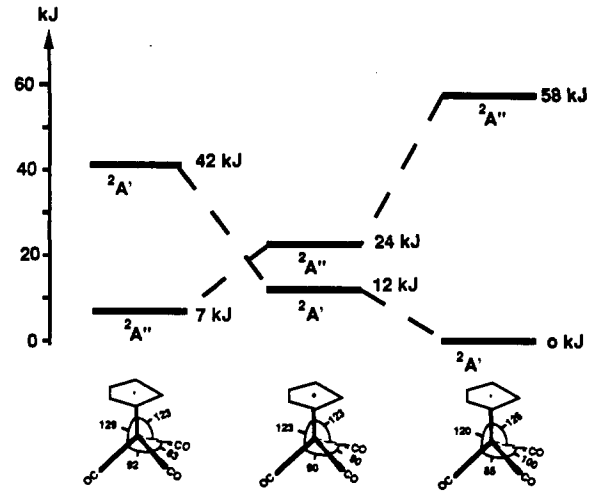


Figure 9. Relative energies of the $^2$A′ and $^2$A″ states of $\{\eta^5\text{-}C_5H_5Cr(CO)_3\}$ in conformations **7**, **9**, and **10**. The energy of the $^2$A′ state of conformation **9** has been set to zero.

for the separation of the ground and excited states from $2\lambda/\Delta g_{zz}$, where $\lambda$ is the spin–orbit interaction constant for $Cr^+$, 220 $cm^{-1}$.[26] The result of this somewhat simplistic calculation is 3700 $cm^{-1}$, in good agreement with the theoretical estimate with the a′–a″ separation (see below).

The accord between theory and experiment for this group of 17-electron radicals is most gratifying. Nevertheless, a difficulty remains to be resolved relating to the rhombic nature of the **g** tensors established for all four species. This observation is in conflict with the theoretical prediction of chromium orbital contributions of $3d_{xy}$ to a″ and of $3d_{z^2} + 3d_{x^2-y^2}$ to a′, since such compositions can only lead to an axial **g** tensor. However, quite small components of the remaining chromium orbitals ($3d_{xz}$ and $3d_{yz}$) may be sufficient to introduce significant asymmetry into the tensor without greatly affecting the energies of the molecular orbitals. We are, unfortunately, unable to calculate EPR spectra from the theoretically derived molecular orbitals discussed in the following section.

**Theoretical Calculations.** We have up to now, in connection with our interpretations of the EPR spectra, discussed the electronic structures of the chromium-centered radicals in rather qualitative terms, based on the schematic energy level diagram of Figure 7. We shall now present a more detailed discussion based on quantitative HFS calculations. Calculated energies for the highest occupied and the lowest unoccupied molecular orbitals of $\{\eta^5\text{-}C_5H_5Cr(CO)_3\}$ are shown to the left in Figure 8 for the case in which all OC–Cr–CO bond angles are equal to 91°. The levels in Figure 8 are labeled, as in Figure 7, according to the $C_s$ point group symmetry of this compound (**1**). The two levels of lowest

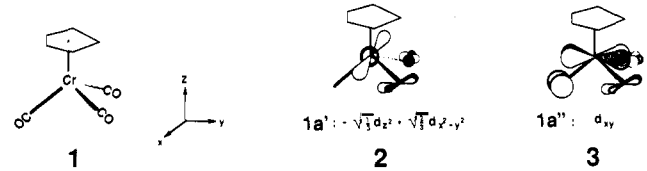


energy, 1a′ (**2**) and 1a″ (**3**), are represented by d-based chromium orbitals, which are involved in a stabilizing interaction with the $\pi^*$ CO orbitals.

At slightly higher energy is another metal-based d orbital, 2a′ (**4**), which exhibits a destabilizing interaction with the occupied $C_5H_5$ orbitals and is again stabilized by interactions with the $\pi^*$ orbitals on the CO ligands. We have finally at yet higher energy 3a′ (**5**), represented by $3d_{yz}$, and 2a″ (**6**), represented by $3d_{xz}$. These latter orbitals both exhibit strong antibonding $\pi$ interactions with occupied orbitals on the $C_5H_5$ ligand.

It follows from our discussion that the energies of the orbitals in Figure 8 increase with the degree of antibonding interaction between the metal-based d component and occupied orbitals on

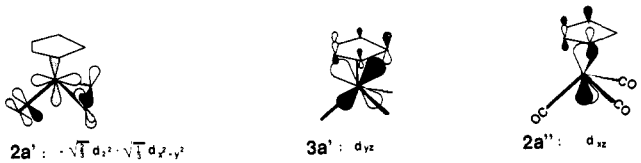


4 5 6

the $C_5H_5$ ring. We find, in accordance with Figure 8, that the electronic ground state for **1** in the symmetrical conformation **7**, where OC–Cr–CO = 91°, has the configuration $(1a')^2(1a'')^2(2a')$,

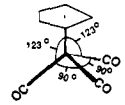

**7**

of $^2A'$ symmetry. The first excited state $^2A''$, with a $(1a')^2(2a')^2(1a'')$ configuration, is, however, only about 12 kJ mol$^{-1}$ higher in energy (Figure 9).

Geometry optimizations of **1** for the two states $^2A'$ and $^2A''$, where the angles $\phi_1$, $\phi_2$, $\Phi_1$, and $\Phi_2$ of **8** were allowed to relax under $C_s$ constraints, resulted in the structures **9** and **10** for $^2A'$ and $^2A''$, respectively. The equilibrium structure **9** for the $^2A'$ state exhibits, compared to **7**, an opening of the angle $\Phi_2$ from

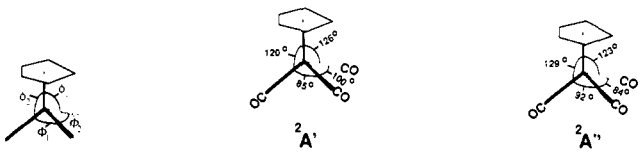


8 9 10

90° to 100°. This increase in $\Phi_2$ enhances the stability of the fully occupied 1a′ (**2**) and 1a″ (**3**) orbitals by increasing the $\pi$ back-donation through increases in the overlap between the d orbitals and the $\pi^*$ combinations on the symmetry-equivalent CO ligands. The singly occupied 2a′ orbital (**4**) is at the same time destabilized by a decrease in the $\pi$ back-donation. The change in the $\phi_2$ angle (**8**) from 123° to 120° is also seen to stabilize the fully occupied 1a″ (**3**) orbital while destabilizing the singly occupied 2a′ orbital (**4**) through changes in the $\pi$ back-donation.

The $^2A''$ state was found to have an equilibrium structure (**10**) in which $\Phi_2$ has been closed, compared to **7**, from 90° to 84°. This decrease will, through changes in $\pi$ back-donation, stabilize the now fully occupied 2a′ orbital (**4**) whereas the singly occupied 1a″ orbital (**3**) and the fully occupied 1a′ (**2**) orbital are somewhat destabilized. The change in the angle $\phi_2$ (**8**) from 123° to 129° will further stabilize 2a′ (**4**) while destabilizing 1a″ (**3**).

We present in Figure 9 the relative energies of the $^2A''$ and $^2A'$ states in the conformations **7**, **9**, and **10**. It follows from Figure 9 that the $^2A'$ state of conformation **9** is lower in energy than the $^2A''$ state of conformation **10** by only about 7 kJ mol$^{-1}$. Further, the activation energy for interconversion between $^2A'$ of conformation **9** and $^2A''$ of conformation **10** can be estimated to be about 20 kJ mol$^{-1}$.

The structure of $\{\eta^5\text{-}C_5H_5Cr(CO)_3\}$ has not been determined experimentally, but earlier EPR studies[3a,b] indicated a $^2A'$ ground state in contrast to the $^2A''$ ground state found in this study for $\{\eta^5\text{-}C_5Me_5Cr(CO)_3\}$. Our calculations suggest that $\{\eta^5\text{-}C_5H_5Cr(CO)_3\}$ should be present in both states in the gas phase and that the relative concentrations of the two states in condensed media may well be sensitive to the local environment.

We have also carried out calculations on $\{\eta^5\text{-}C_5H_5Cr(CO)_2(PH_3)\}$ (**11**) by replacing the unique CO ligand of **1** with a $PH_3$ group. An orbital level diagram is given to the right in Figure

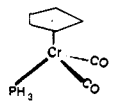

**11**

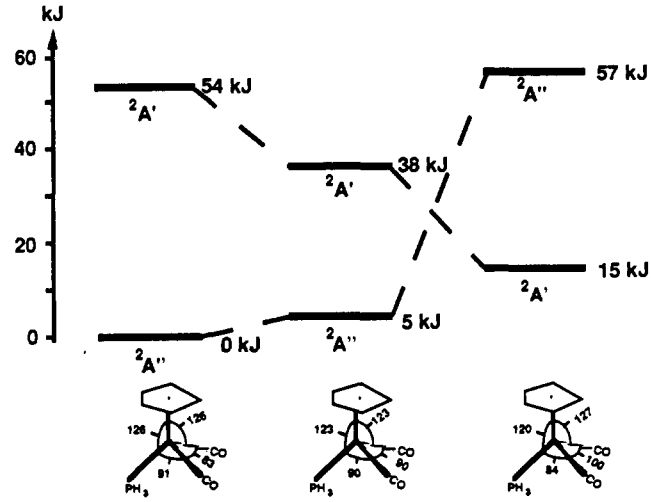


**Figure 10.** Relative energies of the $^2A'$ and $^2A''$ states of $\{\eta^5\text{-}C_5H_5Cr(CO)_2(PH_3)\}$ in conformations **14** and **15**, as well as in the "symmetric geometry" of **11**. The energy of the $^2A''$ state of conformation **14** has been set to zero.

8. The orbitals of $\{\eta^5\text{-}C_5H_5Cr(CO)_2(PH_3)\}$ (**11**) are quite similar to those already discussed for $\{\eta^5\text{-}C_5H_5Cr(CO)_3\}$ (**1**) with the notable difference that the $\pi^*$ orbital on $PH_3$ is a much poorer acceptor than the $\pi^*$ orbital of the unique CO ligand of **1**. For this reason, the metal center in **11** carries more charge than that in **1**, with the consequence that the d-based orbitals are of higher energy in **11** due to the greater electron–electron repulsions. The poor acceptor ability of the $\pi^*$ orbital of $PH_3$ also influences the relative ordering of the d-based levels in **11** compared to **1**. In particular, the 1a″ orbital (**13**) in $\{\eta^5\text{-}C_5H_5Cr(CO)(PH_3)\}$ lacks


**12** **13**

the same degree of $\pi$ back-donation as 1a″ (**3**) of $\{\eta^5\text{-}C_5H_5Cr(CO)_3\}$. This decreased back-donation causes 1a″ (**13**) of $\{\eta^5\text{-}C_5H_5Cr(CO)(PH_3)\}$ to be the highest occupied orbital (Figure 8), with the result that **11** in the symmetrical conformation ($\phi_1$, $\phi_2$ = 123°; $\Phi_1$, $\Phi_2$ = 90°) has a $^2A''$ ground state with the configuration $(1a')^2(2a')^2(1a'')$.

We have also optimized the structure of $\{\eta^5\text{-}C_5H_5Cr(CO)_2(PH_3)\}$ for the $^2A''$ (**14**) and $^2A'$ (**15**) states. The deformations in **14** and **15** resemble those of **9** and **10** and can be rationalized in the same way. We present in Figure 10 the energies of the $^2A'$ and $^2A''$ states in conformations **14** and **15**, as well as in the symmetrical geometry (**11**). It follows from Figure 10 that $\{\eta^5\text{-}C_5H_5Cr(CO)_2(PH_3)\}$ has a $^2A''$ ground state with the geometry given by **14**, whereas the $^2A'$ state of conformation **15** is higher


**14** **15**

in energy by about 15 kJ mol$^{-1}$. The activation energy for the interconversion between **14** and **15** may be estimated from Figure 10 to be about 30 kJ mol$^{-1}$.

We have here discussed equilibrium geometries of the radicals $\{\eta^5\text{-}C_5H_5Cr(CO)_2L\}$ (L = CO, $PH_3$) in the $^2A'$ and $^2A''$ states, finding that the former state has a characteristically wide OC–Cr–CO angle of 100° whereas the latter has a closed angle of 80°. We have further, from detailed analyses of the splittings and compositions of the occupied d levels of $\{\eta^5\text{-}C_5H_5Cr(CO)_2L\}$, been

able to rationalize these variations in the OC–Cr–CO bond angles. It should also be noted that the calculated splittings between $^2A'$ and $^2A''$ states for the same optimized geometries (right and left sides of Figures 9 and 10), of between 42 and 58 kJ mol$^{-1}$, are in close agreement with the order-of-magnitude value of 44 kJ mol$^{-1}$ (3700 cm$^{-1}$) deduced from the EPR experiment (see above).

Interestingly, the $^2A'$ and $^2A''$ states of the radicals $\{\eta^5\text{-}C_5H_5Cr(CO)_2L\}$ in their respective ground state geometries were found to be very close in energy (7–15 kJ mol$^{-1}$), indicating that both might be present in the gas phase. Moreover, because of this close proximity, their relative energies in condensed media may well be sensitive to the local environment. The present EPR study would indicate that both $\{\eta^5\text{-}C_5Me_5Cr(CO)_3\}$ and $\{\eta^5\text{-}C_5Me_5Cr(CO)_2(PMe_3)\}$ adopt $^2A''$ ground states when doped into the diamagnetic manganese analogues.

**Comparisons with Isoelectronic Systems.** There are very few examples of other types of "piano-stool", 17-electron complexes for which complementary EPR and/or crystal structure data have been analyzed in detail.[1] However, several cationic chromium complexes of the type $\{(\eta^6\text{-arene})Cr(CO)_2L^+\}$ (arene = benzene, mesitylene, $C_6Me_6$, biphenyl; L = CO, $PPh_3$)[33] have been synthesized via one-electron oxidation of the corresponding 18-electron analogues. While no crystal structure data are as yet available, low temperatures are necessary to obtain resolved EPR spectra. Interestingly, the spectra of two phosphine-substituted derivatives exhibit highly anisotropic $g$ values ($\simeq$2.10, $\simeq$2.03, $\simeq$1.99[33b]), very similar to the $g$ values obtained here for the $\eta^5\text{-}C_5R_5Cr$ system (Table VIII); the phosphorus hyperfine couplings are also comparable.

In contrast, although the 17-electron tris(pyrazolyl)borate–molybdenum complex $TpMo(CO)_3$ is also believed to be a Jahn–Teller molecule, its X-ray crystal structure shows that the $Mo(CO)_3$ moiety of this molecule exhibits local $C_{3v}$ symmetry.[34] Also in contrast to the $\eta^5\text{-}C_5R_5Cr$ system studied here is a series of (tetaphenylbutadiene)iron complexes of the type $\{(\eta^4\text{-}C_4Ph_4)Fe(CO)_{3-n}L_n^+\}$ (L = CO, tertiary phosphine; $n$ = 1, 2).[35] While the EPR spectra of several of these complexes are significantly broadened at room temperature but exhibit highly anisotropic $g$ values at lower temperatures, the crystal structure of $\{\eta^4\text{-}C_4Ph_4Fe(CO)[P(OME)_3]^+\}$ shows that this complex assumes P–Fe–P and P–Fe–CO angles of 97.3 (1)° and 89.7 (2)°, 95.4 (3)°, respectively,[35b] quite different from the corresponding bond angles of the chromium system. Indeed, it is suggested that the anticipated Jahn–Teller distortion is manifested in this iron system by ring tilting.[35b]

The closest analogy to the chromium-centered radicals discussed here is provided by the isoelectronic series of low-spin manganese(II) complexes of the type $\{(\eta^5\text{-dienyl})Mn(CO)_{3-n}L_n^+\}$ (L = tertiary phosphine; $n$ = 1, 2),[27,36] the powder EPR spectra of which have been examined in great detail recently by Pike, Rieger, and Rieger.[27] Such spectra do not, of course, provide the absolute directional information of a single-crystal study, so that the principal tensor directions can only be inferred for the molecules. However, the results and conclusions of the powder study show very close correspondence with those presented here. In the one case of a precisely isoelectronic radical, $\{\eta^5\text{-}C_5H_5Mn(CO)_2(PPh_3)^+\}$, the principal $g$ values and the isotropic $^{31}P$ coupling are very close to those given in Table VIII for the neutral chromium analogue. The slightly greater departures of the $g$ values from the free-spin value for the manganese species are, in fact, expected because of the slightly larger spin orbit coupling[26] of $Mn^+$ compared to $Cr^0$. Most interesting of all, it was concluded that the ground state of the manganese cation radicals was sensitive to subtle changes in ligation, being either $^2A'$ or $^2A''$ in $C_s$ symmetry; in the case of $\{\eta^5\text{-}C_5H_5Mn(CO)_2(PPh_3)^+\}$, the antisymmetric representation was assigned to the ground state, in agreement with our conclusion for $\{\eta^5\text{-}C_5H_5Cr(CO)_2(PPh_3)\}$.

**Acknowledgment.** The Natural Sciences and Engineering Research Council is thanked for operating grants to S.F., M.C.B., and T.Z. and for a graduate scholarship to J.H.M. We are also indebted to Dr. Phil Rieger, of Brown University, for the provision of a preprint of related research prior to publication and for drawing to our attention a glaring omission from the original manuscript.

**Supplementary Material Available:** Tables of positional parameters and temperature factors for $\eta^5\text{-}C_5Me_5Mn(CO)_3$, $\eta^5\text{-}C_5Me_5Mn(CO)_2(PMe_3)$, and $\{\eta^5\text{-}C_5Me_5Cr(CO)_2(PMe_3)\}$ (8 pages). Ordering information is given on any current masthead page.

(33) (a) Connelly, N. G.; Demidowicz, Z.; Kelly, R. L. *J. Chem. Soc., Dalton Trans.* **1975**, 2335. (b) Van Order, N.; Geiger, W. E.; Bitterwolf, T. E.; Rheingold, A. L. *J. Am. Chem. Soc.* **1987**, *109*, 5680. (c) Doxsee, K. M.; Grubbs, R. H.; Anson, F. C. *J Am. Chem. Soc.* **1984**, *106*, 7819. (d) Zoski, C. G.; Sweigart, D. A.; Stone, N. J.; Rieger, P. H.; Mocellin, E.; Mann, T. F.; Mann, D. R.; Gosser, D. K.; Doeff, M. M.; Bond, A. M. *J. Am. Chem. Soc.* **1988**, *110*, 2109.

(34) Curtis, M. D.; Shiu, K.-B.; Butler, W. M.; Huffman, J. C. *J. Am. Chem. Soc.* **1986**, *108*, 3335.

(35) (a) Connelly, N. G.; Kelly, R. L.; Whitely, M. W. *J. Chem. Soc., Dalton Trans.* **1981**, 34. (b) Orpen, A. G.; Connelly, N. G.; Whitely, M. W.; Woodward, P. *J. Chem. Soc., Dalton Trans.* **1989**, *1751*.

(36) (a) Connelly, N. G.; Kitchen, M. D. *J. Chem. Soc., Dalton Trans.* **1977**, 931. (b) Connelly, N. G.; Freeman, M. J.; Orpen, A. G.; Sheehan, A. R.; Sheridan, J. B.; Sweigart, D. A. *J. Chem. Soc., Dalton Trans.* **1985**, 1019.